Electrochemical properties of a liquid-crystalline mixed fullerene–ferrocene material and related species

Maurizio Carano,[a] Thierry Chuard,[b] Robert Deschenaux,*[b] Michael Even,[b] Massimo Marcaccio,[a] Francesco Paolucci,*[a] Maurizio Prato[c] and Sergio Roffia[a]

[a]Dipartimento di Chimica "G. Ciamician", Università degli Studi di Bologna, Via Selmi, 2, 40126 Bologna, Italy. E-mail: paolucci@ciam.unibo.it; Fax: 00 39 051 209-9456
[b]Institut de Chimie, Université de Neuchâtel, Avenue de Bellevaux 51, Case postale 2, 2007 Neuchâtel, Switzerland. E-mail: robert.deschenaux@unine.ch
[c]Dipartimento di Scienze Farmaceutiche, Università di Trieste, Piazzale Europa 1, 34127 Trieste, Italy

The electrochemical properties of a fullerene–ferrocene liquid crystal are reported. The electrochemical study was carried out under strictly aprotic conditions: a total of seven reduction peaks were detected in the negative potential region, and two oxidation peaks in the positive potential one. Comparison of the data with those obtained from suitable model compounds (*i.e.*, analogous fullerene- or ferrocene-free materials) has allowed the assignment of all reduction and oxidation steps. The CV study evidenced the occurrence of a fast follow-up chemical reaction coupled to the third (at 25 °C) or fourth (at −60 °C) reduction of either **1** or **3**. Such a reaction, presumably related to the cleavage of one of the cyclopropane bonds, is quantitatively reversed upon re-oxidation. Conversely, under bulk electrolysis conditions (second reduction), the species undergo the retro-Bingel reaction, *i.e.* the irreversible removal of the bis(alkoxycarbonyl)methano adducts to give the parent C_{60}.

Introduction

The synthesis and study of multifunctional materials represent a field of intense research activity. In fact, the role played by two or more compounds may well be performed by one single multicomponent molecule (each component can be considered as an active subunit). Electroactive[1] or photoactive[2] liquid crystals belong to the latter class of materials and are of high interest because of the possibility of tuning the mesomorphic and physical properties. If specific properties are to be exploited within liquid-crystalline assemblies, the choice of the subunits is of prime importance.

Fullerene (C_{60}) is a unique electroactive material; it can reversibly accept up to six electrons.[3] Therefore, incorporation of C_{60} into liquid crystals offers the possibility of combining the efficient acceptor characteristics of C_{60} with the anisotropy of liquid crystals.

Three synthetic strategies have been developed in order to design fullerene-containing liquid crystals: 1) addition of liquid-crystalline malonates to C_{60}[4] (leading to methanofullerene derivatives[5]), 2) 1,3-dipolar cycloaddition of liquid-crystalline aldehydes and sarcosine to C_{60}[6] (leading to fulleropyrrolidines[7]), and 3) formation of a complex from a liquid-crystalline cyclotriveratrylene (CTV) and C_{60}.[8]

Mixed fullerene–ferrocene liquid crystals are interesting materials from the point of view of electrochemical properties. Indeed, such compounds associate an electron acceptor subunit (fullerene) and an electron donor subunit (ferrocene). Combination of these two subunits within the same molecular framework could open the doors for the elaboration of new switchable materials: switching between the ferrocene and ferrocenium species could be performed either chemically, as already demonstrated,[1] or photochemically (photoinduced electron transfer in fullerene–ferrocene dyads has been successfully carried out[9]).

Recently, we reported the synthesis, liquid-crystalline behaviour, supramolecular organization, and photoinduced electron transfer of **1**.[4b,e]

We report, herein, the detailed electrochemical behaviour of **1–3**. Compounds **2**[4b,e] and **3**[4a] have been used as model compounds as they lack either the fullerene (*i.e.* **2**) or ferrocene (*i.e.* **3**) subunit. Note that **1–3** displayed smectic A phases.
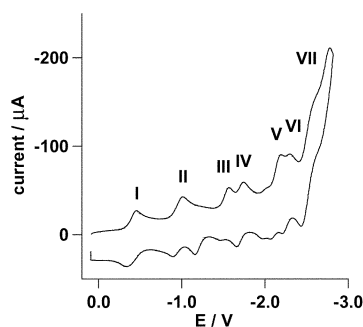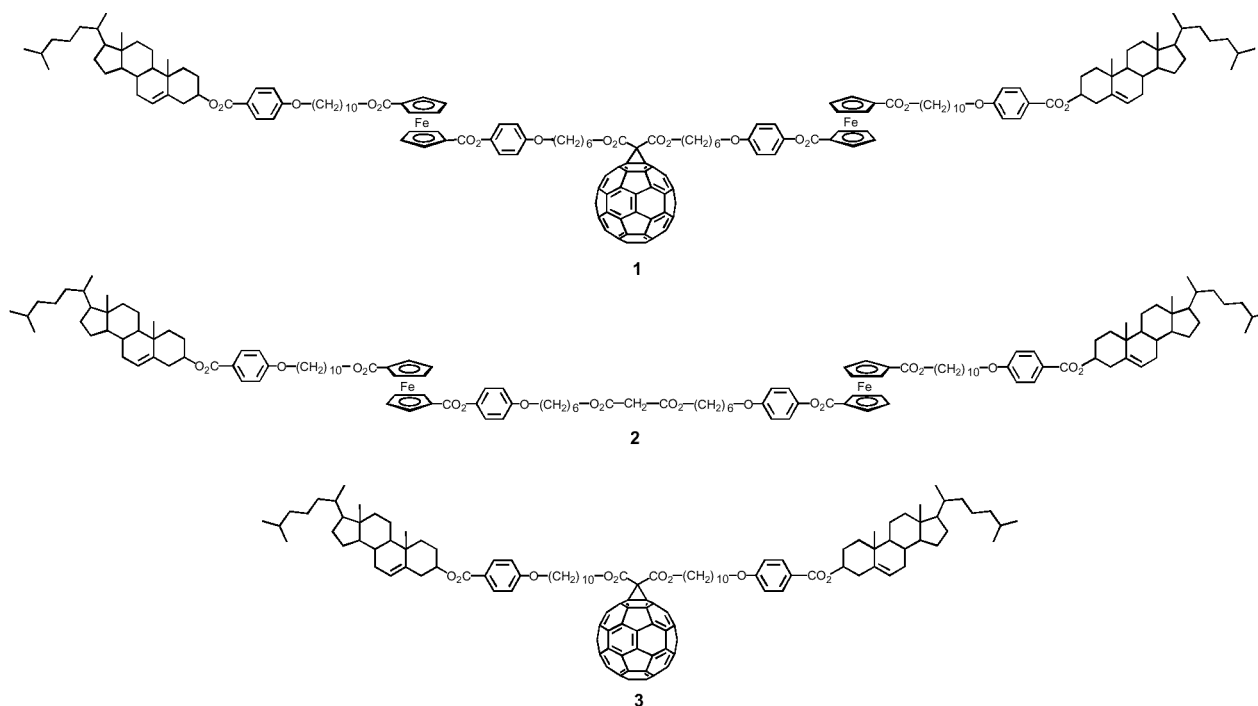

Fig. 1 CV curve of a 0.5 mM **1**–0.05 M TBAH–THF solution. Scan rate: 0.5 V s⁻¹; T = 25 °C; working electrode: platinum.

Results and discussion

The electrochemical properties of compounds **1–3** were investigated under strictly aprotic conditions obtained by employing vacuum techniques and chemical pre-treatment of the solvents for the careful exclusion of water from the electrochemical cell.[10] Dichloromethane (DCM) was used for investigating the region of positive potentials while tetrahydrofuran (THF) was used for investigating the region of of negative potentials. The latter solvent allows a very wide negative potential window and liquid-state temperature range to be analysed.[10] Furthermore, DCM can react with fullerene trianions to form methanofullerenes.[11] The cyclic voltammetric (CV) curve of a 0.5 mM solution of **1** in THF, at 25 °C, is rather complex (Fig. 1). The CV curve is characterised by a large number of reduction peaks (denoted by Roman numbers) displaying either reversible or irreversible features and different heights. In particular, peak VII comprises two multielectronic peaks occurring at similar potentials, while peak V corresponds to the exchange of two electrons per molecule.[12] The curve also evidences the occurrence of chemical reactions coupled to some of the redox processes that are responsible for the presence of extra anodic peaks in the reverse scan. The complex pattern of the CV curve of **1** was not unexpected due to the presence of several electroactive units, namely the methanofullerene moiety, the ferrocene units and the aromatic ester groups. Additional complexity arises from the known reactivity of multiply-reduced bis(alkoxycarbonyl)methanofullerene derivatives.[13] Conversely, the CV curve of a 0.5 mM solution of **1** in DCM shows only two oxidation processes: the first one corresponds to the reversible exchange of two electrons (with $E = 0.96$ V), attributed to the two ferrocenyl units, and the second one corresponds to an irreversible one-electron
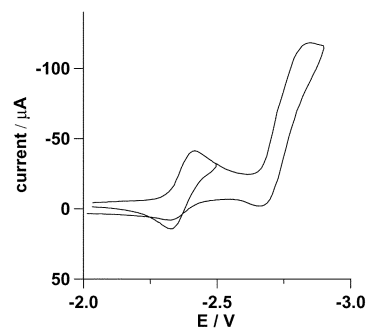

Fig. 2 CV curve of a 0.5 mM **2**–0.05 M TBAH–THF solution. Scan rate: 0.5 V s^{-1}; $T = 25$ °C; working electrode: platinum.

oxidation, with $E_p = 1.68$ V (at 0.5 V s^{-1}), located on the fullerene unit.[14]

In order to localize and characterize the redox sites of **1**, compounds **2** and **3** were studied. Materials **2** and **3** are suitable models of **1** since they contain, within similar molecular frameworks, the electroactive moieties of **1**.

The CV curve of **2**, obtained under the conditions of Fig. 1, is shown in Fig. 2. As expected, the curve is simplified with respect to that of **1** and shows only two reduction processes and with very different heights. The first peak is fully reversible and corresponds to the exchange of two electrons at close potentials ($E = -2.38$ V, close to the corresponding value for peak V in Fig. 1, see Table 1), while the second one is only partly reversible ($E_p = -2.74$ V) and corresponds to the exchange of four electrons.[12] The reversibility of the first peak decreases when the forward scan also includes the second peak. Finally, in line with the oxidative behavior of **1**, a reversible

Table 1 E (E_p for irreversible peaks)/V *vs.* SCE for compounds **1–3**. Scan rate: 0.5 V s^{-1}; $T = 25$ °C

Compound	Oxidations^a		Reductions^b							
1	1.68^c	0.96^d	−0.41	−0.98	−1.55^c	−1.75	−2.04	−2.33^d	−2.40	−2.67^{c,e}
2		0.95^d						−2.38^d		−2.74^{c,e}
3	1.66^c		−0.41	−0.96	−1.53^c	−1.70	−2.00		−2.28	−2.55^{c,e}

^{a}0.5 mM in DCM–0.05 M TBAH. ^{b}Solvent: THF. ^{c}Irreversible peak. ^{d}Ferrocenyl-centered bielectronic peak. ^{e}Multielectronic peak involving the aromatic ester groups. In italics: reduction processes involving the product yielding from the third irreversible reduction of the fullerene moiety (see text).

anodic peak is observed in DCM corresponding to a two-electron oxidation process with an apparent $E = 0.95$ V. The observed electrochemical processes were attributed to the reduction (-2.38 V) and oxidation (0.95 V) of the two equivalent ferrocenyl moieties, while the four-electron peak (-2.74 V), occurring at rather negative potentials, may be attributed to the chemically-irreversible reduction of the four aromatic ester groups. The fact that two of these groups are conjugated with the ferrocenyl moieties may explain why the reduction of the latter becomes less reversible when the cathodic scan also includes the last irreversible reduction peak (Fig. 2).

The CV curve of **3** in THF (Fig. 3) shows a complex pattern, similar to that observed for **1**. The multielectronic peak occurring at very negative potentials ($E_p = -2.55$ V) is, analogously to the preceding species, attributed to the aromatic ester groups. The two-electron reversible reduction peak (peak V) of Fig. 1 is missing in this case, confirming the attribution of that peak to the reduction, in **1**, of the ferrocenyl units. The remaining peaks in Fig. 3 are therefore attributed to the fullerene moiety. As anticipated above, the presence of irreversible cathodic peaks (the third one, for instance) and of the extra anodic peak (at *ca.* -1.1 V) in the reverse scan prove the occurrence of a follow-up chemical reaction coupled to the fullerene-centered reductions. Further details relative to such an EC (electrochemical–chemical) mechanism (involving either **3** or **1**) were obtained by performing CV experiments as a function of scan rate, temperature and reversal potential. The CV curves of **3**, obtained under the conditions of Fig. 3, and including a decreasing number of reduction peaks in the scan are shown in Figs. 4a and 4b. Their analysis evidences that (i) the extra anodic peak at -1.15 V is due to a novel species formed following the third (irreversible) reduction of the fullerene derivative; (ii) the follow-up chemical reaction responsible for the behavior described in (i) is fully reversed upon performing the oxidation scan [a second cathodic scan carried out without the renewal of the diffusion layer (Fig. 4a) shows in fact the same CV pattern as observed in the first scan]; (iii) the first two reductions are reversible under the conditions of Fig. 4 and at scan rates as slow as 0.05 V s^{-1}. Conversely, a cathodic counterpart of the anodic peak at -1.15 V was detected by reversing the anodic scan at -1.0 V, the two peaks comprising a reversible redox couple with $E = -1.18$ V. By increasing the scan rate (up to 200 V s^{-1}), the third peak height increased sensitively at the expense of the fourth one, although the suppression of the latter peak and the reversibility of the third one was not reached. Such a behavior implies that the fourth peak ($E = -1.70$ V) has to be attributed to the product that is formed from the chemical reaction coupled to the third reduction of **3**, rather than to the pristine fullerene derivative. A more reversible behavior relative to the first three reductions was obtained by lowering the temperature, as shown in Figs. 5a and 5b. The curve in Fig. 5b exhibits a reversible pattern where
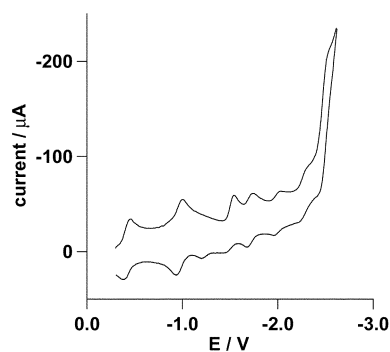
only small traces of the chemical species responsible for the anodic peak at -1.15 V (compare with Fig. 4b) are observed. Comparison of the CV curves in Figs. 4 and 5 suggests that the reactivity observed at the level of the trianion at high temperature is transferred, at low temperature, to the level of the fourth reduction. Interestingly, in Fig. 5a, an extra anodic peak is observed in the reverse scan (at *ca.* -1.75 V) that coincides with the anodic partner of the fourth reduction peak
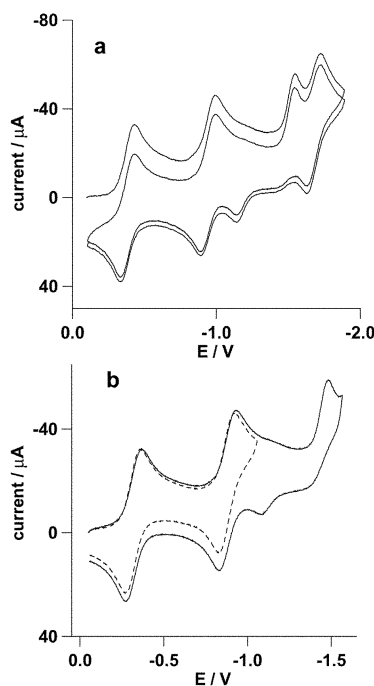

Fig. 4 CV curves of a 0.5 mM **3**–0.05 M TBAH–THF solution as a function of reversal potential. Conditions as in Fig. 3.

Fig. 3 CV curve of a 0.5 mM **3**–0.05 M TBAH–THF solution. Scan rate: 0.5 V s^{-1}; $T = 25$ °C. Working electrode: platinum.
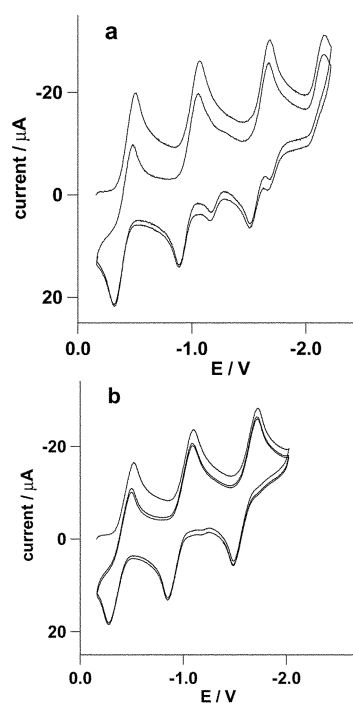

Fig. 5 CV curves of a 0.5 mM **3**–0.05 M TBAH–THF solution as a function of reversal potential. Scan rate: 0.5 V s^{-1}; $T = -60$ °C. Working electrode: platinum.

observed in the curve at high temperature (Fig. 4a), substantiating the hypothesis that the latter peak should not be attributed to the pristine fullerene derivative. Finally, analogously to what is observed at high temperature, the chemical reaction coupled to the fourth reduction is fully reversed upon re-oxidation, as shown in the second and subsequent scans, where the CV pattern consistently remains the same as in the first scan.

The elucidation of the electrode kinetic mechanism evidenced by the CV experiments is outside the scope of the present paper and will be the subject of future work.[15] On the other hand, the stability of **1** under reductive conditions is important in view of its application as a photoactive molecular device. In fact, it has been recently proposed that the intramolecular electron transfer between the ferrocene and fullerene units represents the major deactivation pathway of the electronically-excited **1**.[4e] The charge-separated state, comprising the ferrocenyl radical cation and the fullerene-centered radical anion, lives a few hundreds of nanoseconds,[4e] thus preventing any chemical degradation of the reduced fullerene moiety. However, as strategies are developed for prolonging such charge-separated state lifetimes,[16] thus making the stored chemical energy available for useful applications, the stability of the reduced **1** over longer time scales, such as those typical of electrochemical experiments (*i.e.* milliseconds to minutes), becomes a relevant issue. Important results, in this respect, obtained by the above CV investigations, are (i) that the reaction responsible for the irreversible behavior of **1** and **3** is only triggered by the injection of at least three (at 25 °C) or four (at −60 °C) electrons; (ii) that the reaction coupled to the multiple reduction of the fullerene derivatives is reversed, in either **1** or **3**, upon their re-oxidation, using relatively low scan rates. This implies that the transient chemical species generated by the reduction of **1** and **3**, presumably to be identified by the corresponding fullerene derivatives in which one of the cyclopropane bonds has been cleaved,[13a,b,17] are stable in the relatively long time scale of CV. Such was not the case when controlled potential electrolysis was carried out in benzonitrile after the second reduction of either **1** or **3**. A 0.2 mM **1**–0.05 M TBAH–benzonitrile solution was electrolyzed at −0.7 V. This potential corresponds to the first reduction of the species. As the electrolysis proceeded, consuming on the whole one electron per molecule, the typical absorption features in the visible and NIR regions of the monoanion of the fullerene derivatives[18] appeared and developed in the spectra: the NIR absorption maximum occurred at 1033 nm (Fig. 6). The electrolyzed solution kept under inert atmosphere (Ar) was stable for several hours. The potential was then set at −1.2 V
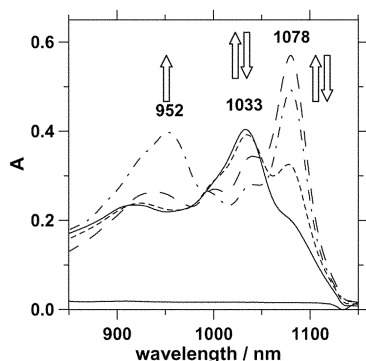
that corresponds to the second fullerene-centered reduction of **1**. Instead of the conversion of the monoanion spectrum to that typical of doubly-reduced fullerene derivatives,[18] a shoulder at 1078 nm appeared and developed into an intense band during the electrolysis, at the expense of the absorption maximum at 1033 nm (Fig. 6). After consuming an additional charge well above one electron per molecule, a novel band at 952 nm developed, while that at 1078 nm decreased. The bands at 1078 and 952 nm were identified as due to the pristine C_{60} mono- and dianion respectively, as reported, under identical conditions, in the literature.[18] The complex spectral evolution observed during the electrolysis of **1** and the formation of pristine C_{60}, are in line with the reported behavior for this class of fullerene derivatives: the species undergoes the so-called retro-Bingel reaction, that consists of the irreversible removal, under bulk electrolysis conditions, of bis(alkoxycarbonyl)methano adducts to give the parent C_{60}.[13]

Conclusion

Both fullerene- and ferrocene-centered oxidation and reduction processes were observed in **1**. For both **1** and **3**, in the CV experiments carried out at 25 °C, the third reduction process, centered on the fullerene moiety, triggers a fast follow-up reaction that is, however, fully reversed upon reoxidation of the species. Furthermore, at very negative potentials, multi-electron and irreversible reduction processes are observed that are attributed to the aromatic moieties within the liquid-crystalline structure. The irreversible removal of bis(alkoxycarbonyl)-methano adducts to give the parent C_{60} (retro-Bingel reaction) was obtained under bulk electrolysis conditions.

Experimental

Materials. The synthesis and liquid-crystalline properties of **1–3** have been described elsewhere.[4a,b,e] All materials were reagent grade chemicals. Tetrabutylammonium hexafluorophosphate (TBAH, puriss from FLUKA) was used as supporting electrolyte as received. CH_2Cl_2 (DCM, puriss. from Fluka) was transferred, under argon, from the original air-tight container into a Schlenk flask containing activated 4 Å molecular sieves and kept under vacuum prior to use. Tetrahydrofuran (THF, LiChrosolv, Merck) was treated according to a procedure described elsewhere.[10] Benzonitrile (puriss. from Fluka) was used as received. For the cyclic voltammetry experiments, the solvent was distilled into the electrochemical cell, prior to use, using a trap-to-trap procedure.

Electrochemical instrumentation and measurements. The cyclic voltammetry experiments were carried out according to procedures described elsewhere.[10] Potentials were measured with respect to the ferrocene standard and are always referred to the saturated calomel electrode (SCE). *E* values correspond to $(E_{pc} + E_{pa})/2$ from CV. For irreversible peaks, the peak potential, E_p, is given, measured at 0.5 V s^{-1}. Ferrocene was also used as an internal standard for checking the electrochemical reversibility of a redox couple.

Voltammograms were recorded with an AMEL Model 552 potentiostat controlled by either an AMEL Model 568 function generator or an ELCHEMA Model FG-206F. Data acquisition was performed by a Nicolet Model 3091 digital oscilloscope interfaced to a PC. Temperature control was accomplished within 0.1 °C with a Lauda 2000 thermostat. Potential-controlled bulk electrolysis was carried out in a three-compartment electrochemical cell with both the SCE reference electrode and the platinum spiral counter electrode separated from the working electrode compartment by sintered glass frits. The working electrode was a large area platinum gauze. The electrolysis charge was measured by an AMEL Model 731

Fig. 6 NIR spectral changes during electrolysis of a 0.2 mM **1**–0.05 M TBAH–benzonitrile solution; *T* = 25 °C; working electrode: platinum gauze. The full lines correspond either to the starting solution (bottom) or to the electrolysed solution after 1 electron per molecule (obtained at −0.7 V). The dash-dot line corresponds to an electrolysis charge above 2 electron per molecule (at −1.2 V) and the dashed lines to intermediate charges (see text).

digital integrator. Absorption spectra were taken using a VARIAN Cary 5E UV-VIS-NIR spectrophotometer.

Acknowledgement

References

1   (*a*) R. Deschenaux, M. Schweissguth and A.-M. Levelut, *Chem. Commun.*, 1996, 1275; (*b*) R. Deschenaux, M. Schweissguth, M. T. Vilches, A.-M. Levelut, D. Hautot, G. J. Long and D. Luneau, *Organometallics*, 1999, **18**, 5553.

2   (*a*) M. Zhang and G. B. Schuster, *J. Am. Chem. Soc.*, 1994, **116**, 4858; (*b*) L. Dinescu, K. E. Maly and R. P. Lemieux, *J. Mater. Chem.*, 1999, **9**, 1679; (*c*) B. L. Feringa, R. A. van Delden, N. Koumura and E. M. Geertsema, *Chem. Rev.*, 2000, **100**, 1789.

3   (*a*) Q. Xie, E. Pérez-Cordero and L. Echegoyen, *J. Am. Chem. Soc.*, 1992, **114**, 3978; (*b*) L. Echegoyen and L. E. Echegoyen, *Acc. Chem. Res.*, 1998, **31**, 593.

4   (*a*) T. Chuard and R. Deschenaux, *Helv. Chim. Acta*, 1996, **79**, 736; (*b*) R. Deschenaux, M. Even and D. Guillon, *Chem. Commun.*, 1998, 537; (*c*) B. Dardel, R. Deschenaux, M. Even and E. Serrano, *Macromolecules*, 1999, **32**, 5193; (*d*) T. Chuard, R. Deschenaux, A. Hirsch and H. Schönberger, *Chem. Commun.*, 1999, 2103; (*e*) M. Even, B. Heinrich, D. Guillon, D. M. Guldi, M. Prato and R. Deschenaux, *Chem. Eur. J.*, 2001, **7**, 2595; (*f*) B. Dardel, D. Guillon, B. Heinrich and R. Deschenaux, *J. Mater. Chem.*, 2001, **11**, 2814; (*g*) N. Tirelli, F. Cardullo, T. Habischer, U. W. Suter and F. Diederich, *J. Chem. Soc., Perkin Trans. 2*, 2000, 193.

5   C. Bingel, *Chem. Ber.*, 1993, **126**, 1957.

6   S. Campidelli and R. Deschenaux, *Helv. Chim. Acta*, 2001, **84**, 589.

7   M. Prato and M. Maggini, *Acc. Chem. Res.*, 1998, **31**, 519.

8   D. Felder, B. Heinrich, D. Guillon, J.-F. Nicoud and J.-F. Nierengarten, *Chem. Eur. J.*, 2000, **6**, 3501.

9   D. M. Guldi, M. Maggini, G. Scorrano and M. Prato, *J. Am. Chem. Soc.*, 1997, **119**, 974.

10 (*a*) M. Carano, P. Ceroni, L. Mottier, F. Paolucci and S. Roffia, *J. Electrochem. Soc.*, 1999, **146**, 3357; (*b*) S. Cattarin, P. Ceroni, D. M. Guldi, M. Maggini, E. Menna, F. Paolucci, S. Roffia and G. Scorrano, *J. Mater. Chem.*, 1999, **9**, 2743.

11 M. W. J. Beulen and L. Echegoyen, *Chem. Commun.*, 2000, 1065.

12 The evaluation of the charge associated with the various reduction peaks was carried out by the convolutive technique: A. J. Bard and L. R. Faulkner, *Electrochemical Methods; Fundamentals and Applications*, Wiley, New York, 2001, ch. 6. In the case of the CV curves in Figs. 1–3, a multi-step sigmoidal curve is obtained after convolution, where each step is proportional to the number of electrons exchanged in the corresponding redox process.

13 (*a*) M. W. J. Beulen, J. A. Rivera, M. Á. Herranz, Á. Martín-Domenech, N. Martín and L. Echegoyen, *Chem. Commun.*, 2001, 407; (*b*) M. W. J. Beulen, L. Echegoyen, J. A. Rivera, M. Á. Herranz, Á. Martín-Domenech and N. Martín, *Chem. Commun.*, 2000, 917; (*c*) R. Kessinger, J. Crassous, A. Herrmann, M. Rüttiman, L. Echegoyen and F. Diederich, *Angew. Chem., Int. Ed.*, 1998, **37**, 1919.

14 F. Cardullo, P. Seiler, L. Isaacs, J. F. Nierengarten, R. F. Haldimann, F. Diederich, T. Mordasini-Denti, W. Thiel, C. Boudon, J.-P. Gisselbrecht and M. Gross, *Helv. Chim. Acta*, 1997, **80**, 343.

15 M. Carano and L. Echegoyen, unpublished results.

16 (*a*) D. M. Guldi, *Chem. Commun.*, 2000, 321; (*b*) F. Diederich and M. Gómez-López, *Chem. Soc. Rev.*, 1999, **28**, 263.

17 (*a*) B. Knight, N. Martín, T. Ohno, E. Ortí, C. Rovira, J. Veciana, J. Vidal-Gancedo, P. Viruela, R. Viruela and F. Wudl, *J. Am. Chem. Soc.*, 1997, **109**, 9871; (*b*) N. Martín, L. Sánchez, B. Illescas and I. Pérez, *Chem. Rev.*, 1998, **98**, 2527.

18 C. A. Reed and R. D. Bolskar, *Chem. Rev.*, 2000, **100**, 1075.